Detection of FGFR2: FAM76A fusion gene in circulating tumor RNA based on catalytic signal amplification of graphene oxide-coated magnetic nanoparticles

Lena Gorgannezhad,[a,b] Muhammad Umer,[b] Mostafa Kamal Masud,[c] Yusuke Yamauchi,[d] Shahriar Al Hossain,[c] Carlos Salomon,[e,f,g] Richard Kline, [g] Nam-Trung Nguyen,[b] Muhammad J.A. Shiddiky[a,b*]

[a]*School of Environment and Science, Griffith University, Nathan Campus, QLD 4111, Australia*

[b]*Queensland Micro- and Nanotechnology Centre, Griffith University, Nathan Campus, QLD 4111, Australia*

[c]*Australian Institute for Innovative Materials (AIIM), University of Wollongong, Squires Way, Innovation Campus, North Wollongong, NSW 2519, Australia*

[d]*International Center for Materials Nanoarchitectonics, National Institute for Materials Science (NIMS), Japan 1-2-1 Sengen, Tsukuba-city, Ibaraki 305-0047, Japan*

[e]*Exosome Biology Laboratory, Centre for Clinical Diagnostics, University of Queensland Centre for Clinical Research, Royal Brisbane and Women's Hospital, The University of Queensland, Brisbane, QLD, Australia*

[f]*Department of Clinical Biochemistry and Immunology, Faculty of Pharmacy, University of Concepción, Concepción, Chile.*

[g]*Maternal-Fetal Medicine, Department of Obstetrics and Gynecology, Ochsner Clinic Foundation, New Orleans, USA.*

Keywords: Biosensors, Cancer, Fusion Genes, GO coated magnetic Nanoparticles, Liquid Biopsy

*Corresponding author emails: m.shiddiky@griffith.edu.au (MJAS).

(†Electronic supplementary information (ESI) available. See DOI: XXXXXXXX)

Abstract

Circulating tumor nucleic acids (ctNAs) are promising biomarkers for minimally invasive cancer assessment. The FGFR2: FAM76A fusion gene is one of a series of highly promising ovarian cancer biomarkers detectable in ctNAs. Herein, we introduce a new amplification–free electrochemical assay for the detection of FGFR2: FAM76A fusion gene in ctNAs extracted from ovarian cancer patients. The assay relies on the electrocatalytic activity of a new class of superparamagnetic graphene-loaded nonporous iron oxide nanoparticles (GO-NPFe_2O_3). After isolation and purification, the target RNA was directly adsorbed onto the GO-NPFe_2O_3 surface through graphene-RNA affinity interaction. The electrocatalytic signal was achieved by the reduction of surface-attached ruthenium hexaammine(III) chloride which was further enhanced by using the ferri/ferrocyanide redox system. Our assay depicted an excellent detection sensitivity down to 1.0 fM, high specificity and excellent reproducibility (% RSD = < 5%, for n = 3). The analytical performance of our method was validated with standard qRT-PCR analysis. We believe that this newly developed assay would be practically applicable in clinical research.

Introduction

Circulating tumor nucleic acids (ctNAs) have emerged as promising biomarkers for diagnosis, prognosis, treatment response prediction, as well as assessment of tumor stage.[1] As the access to circulating nucleic acids is minimally invasive, ctNA analysis may replace painful, expensive, and time-consuming tumor tissue biopsy.[2] However, ctNA detection is an exigent task primarily due to their extremely low abundance in serum/plasma and low allele frequencies of targeted molecular alterations. Moreover, highly fragmented nature makes their isolation and analysis difficult.[2a]

Somatic genomic rearrangements such as translocation, deletion, or inversion can lead to joining together of previously separate genes. The resulting hybrid or "fusion genes" can induce cancer initiation and progression by altering expression levels, or functionality.[3] Fusion genes are exceptionally powerful cancer biomarkers, as in most cases they are pathognomonic in contrast to other more promiscuous genetic lesions, like point mutations, which can be found in several types of cancers. Fusion genes have been detected in various cancers, such as breast,[4] lung,[5] prostate,[6] and ovarian[7] and have attracted a great deal of attention from the research community in recent years. Ovarian cancer is the seventh most common cancer among females worldwide and causes more than 150,000 deaths annually. Several fusion genes have been identified in ovarian cancer and occur frequently in high-grade serous carcinoma (HG-SC). A previous study identified 45 fusion genes in ovarian cancer, however primarily due to high level of heterogeneity, none of the fusion genes occurred in more than one patients.[8] Nonetheless, transcriptome sequencing has identified fusion genes ESRRAC11or f20[9] and CDKN2D-WDFY2[10] in 15% and 20% of the patients, respectively, thus suggesting some gene fusion events may play a critical role in HG-SC development. Fusion between the exon 17 of FGFR2 gene and the exon 2 FAM76A gene (FGFR2: FAM76A) has also been reported in ovarian cancer, whose expression can cause up to 50% increase in

proliferation of the cultured ovarian cancer cells.[7] Moreover, as it was shown that FGFR2: FAM76A could be detected noninvasively in ctNAs, this gene fusion event can be considered as a promising minimally invasive biomarker for the detection of ovarian cancer.

Current ctNA detection methodologies have largely been limited to polymerase chain reaction (PCR)[11] or sequencing.[12] Though sequencing is robust and sensitive, high cost and long analysis time makes it particularly unsuited for routine clinical use.[13] On the other hand, PCR based methods are amenable to biological interference and require sample preprocessing.[2b] Electrochemical approaches represent attractive alternatives for the analysis of ctNAs owing to their low cost, relatively high sensitivity, specificity and capacity for multiplex detection.[14] Over the past few years, various new electrochemical strategies have been introduced to improve the detection sensitivity of ctNAs, such as DNA concatamer-based biosensor,[15] DNA nanostructure-based biosensor[16] and nanocomposite-based biosensors.[17] Nevertheless, these technologies are partially hampered by the requirements of signals amplification, complex surface modification and necessity of target labeling. Moreover, analysis of patient samples (heterogenous) for target biomarker is challenging using these methodologies due to their limited selectivity. Recently, Kelley et al. reported a novel electrochemical clamp assay using DNA clutch probes (DCPs), which could directly detect mutated circulating nucleic acids in patient serum.[18] Although this elegant approach is enzyme-free and sensitive, the complexity of clamp fabrication limits its broad applications. On the other hand, sensitive and selective label-free electrochemical ctNA sensing platforms based on nanocomposites such as MoS_2/graphene have emerged as a new class of biosensors. For example, Chu et al. used synthetic oligonucleotide probes immobilized on MoS2/graphene nanosheets for the detection of E542K mutation in PIK3CA gene.[17a] Similarly, Koo et al. have reported the detection of prostate cancer specific fusion gene by combining isothermal amplification and label-free readout.[19]

This paper reports a new method for sensitive and specific detection of FGFR2: FAM76A fusion gene via electrocatalytic signal amplification. To the best of our knowledge, this assay is the first amplification-free approach for electrochemical detection of FGFR2:FAM76A fusion gene in ctRNA. To this end, target FGFR2: FAM76A RNA were magnetically isolated and purified using probes complementary to the gene fusion junction. Purified target RNAs were subsequently directly adsorbed onto the graphene surfaces of a GO-NPFe_2O_3 through graphene-RNA affinity interaction followed by electrocatalytic reduction of surface-attached ruthenium hexaammine(III) chloride ($[Ru(NH_3)_6]^{3+}$).. The electrocatalytic signal was further enhanced by using the ferri/ferrocyanide ($[Fe(CN)_6]^{3-/4-}$) system coupled with the $[Ru(NH_3)_6]^{3+/4+}$ system. Our assay was successfully tested in plasma samples of patients with ovarian cancer.

Experimental sections

Reagents and materials

Analytical-grade reagents and chemicals were used in this assay, unless mentioned otherwise. Hexaammineruthenium(III) chloride and phosphate buffer saline (PBS) tablets were obtained from Sigma-Aldrich (Australia). Tris was purchased from VWR Life science (Australia). UltraPure™ DNase/RNase-free distilled water (Invitrogen, Australia) was used throughout. Synthetic RNA, primers and capture probes were obtained from Integrated DNA Technologies (Coralville, IA, USA) and sequences are depicted in Table S1. Screen-printed carbon electrodes (SPCE) (DRP-150) were purchased from DropSens (Spain). In the three-electrode system, working (4 mm diameter), counter and reference electrodes were carbon, platinum and silver-modified respectively.

Synthesis and Characterization of GO-NPFe_2O_3

The synthesis and characterization of GO-NPFe_2O_3 has been reported previously.[20] In brief, the synthesis procedure involves three major steps 1) preparation of graphene oxide using Hummer's method. Sodium nitrate (0.3 g) was dissolved in sulfuric acid solution (10 mL), followed by the addition of nanographite platelet powder. Then, $KMnO_4$ (0.30 g) was mixed with the previous solution. After 1 h of mixing, H_2O_2 (10 mL) was added to the mixture to generate GO sheets. 2) 40 mL solution comprising 3.24 g of $FeCl_3.6H_2O$ and 3.24 g of TSCD was added to a 40 mL solution containing 4.36 g of $Na_4[Fe(CN)_6].10H_2O$. The prepared solution was stirred for 1 h and aged overnight. The Prussian blue (PB) nanoparticles were then achieved by centrifugation. 3) In the last step, GO and PB solutions obtained in previous steps were mixed in the specific weight ratios of 25:75 and were diluted down to 2 $mgmL^{-1}$ by adding water to obtain GO-NPFe_2O_3. Then, the mixture was sonicated, aged for 24 h and dried at room temperature. Finally, the mesoporous GO-NPFe_2O_3 was achieved by calcining the GO/PB powders at 400°C with a heating rate of 1°$Cmin^{-1}$. For characterizing of GO-NPFe_2O_3, SEM, wide-angle XRD and N_2 adsorption-desorption isotherms studies have been performed (see Ref. 28 for details). As discussed in Ref 28, the original 2D morphology of the GO sheet is well preserved while the PB nanoparticles are located within the stacked GO sheets interlayer spacing. The surface area and pore volumes were calculated to be 120.5 m/g and 0.384 cc/g by the BET and BJH methods, respectively.

Study group and samples

Staged samples (cross sectional) were collected at the Ochsner Baptist Medical Center and obtained via The UQ Centre for Clinical research (UQ IRB 2016000300). Plasma samples were obtained in accordance with the declaration of Helsinki and approved by the Ethics Committee

of The University of Queensland and the Ochsner Medical Center (New Orleans, USA). Plasma was separated from whole blood by centrifugation (2000gx 10 min at Room temperature) and stored at -80^{o}C until further analysis. Ovarian cancer samples were collected prospectively and assigned according to the histotype classification (e.g., stage I, and stage III) and stored to -80 ^{0}C in the Biobank units. Only patients with epithelial ovarian cancer high-grade serous subtype (n=5) and benign controls (n=5) were included in this study.

RNA Extraction from Clinical plasma Samples

Total RNA was extracted from 200 µL of each plasma sample using plasma/serum RNA purification mini kit 55000 (Norgen Biotech Corp, Canada) according to the manufacturer's recommendations. The extracted RNA was eluted in 20 µL elution buffer. Nanodrop spectrophotometric analysis (BioLab, Ipswich, MA, USA) was performed to quantify and verify the purity of extracted RNA. The concentration of RNA was recorded in ng/µL and stored at -80^{O}C until assayed.

Probe Hybridization and Magnetic Isolation

In order to perform probe hybridization, extracted total RNA from plasma samples were adjusted to a concentration of 50 ng/µL with 5X saline sodium citrate (SSC) buffer (pH 7). 5 µL of concentration adjusted RNA solution was mixed with 10 µL of 10 µM biotinylated capture probes [(5′-TGA-AAG-GAA-AGG-AAC-**ATA-TGT-TTG-TTT-TAC-A**-3′-Biotin) [Underlined and bold are complementary to FGFR2 and FAM76A sequences, respectively]. The mixture was then heated to 65°C for 2 min for linearization of RNA followed by incubation for 1 h at room temperature to allow capture probe hybridization to the target (FGFR2:FAM76A) RNA. For magnetic isolation, 10 µL of streptavidin-labeled magnetic beads (dynabeads myone streptavidin C1; Invitrogen) were washed twice with washing and

binding (B&W) buffer (10 mM Tris-HCl, pH 7.5; 1 mM EDTA; 2 M NaCl) and re-suspended in 10 µL of B&W buffer solution. The magnetic beads were then added to the solution and incubated for 30 minutes at room temperature. Finally, the magnetic bead attached hybrid probes were isolated using a magnet, washed twice with B&W buffer, and resuspended in 10 µL of RNase-free water. The mixture was then heated for 2 min at 95 °C for release of captured target RNAs, and instantly placed on a magnet to collect the supernatant. 5.0 µL of released target ctRNA was diluted with 10 µL of 5X SSC buffer (pH 7.0) for subsequent electrochemical measurements.

Adsorption of Isolated RNA on modified SPCE

The SPCE was washed with an excess amount of Milli-Q water and positioned onto a permanent magnet in such a way that the working electrode surface was centered to the magnet (Figure S1). 4µg of GO-NPFe_2O_3 nanoparticles were employed on the electrode surface and allowed to attach magnetically. The modified SPCE was then washed with 10 mM PBS to remove unattached or loosely attached particles from the electrode surface before conducting subsequent steps for electrochemical readout.

Electrochemical Detection

CHI650 electrochemical workstation (CH instrument, USA) was used in all the electrochemical experiments. The effective SPCE surface area was determined using the Randles- Sevcik equation (eq. 1) as described previously.[21, 22]

$$i_p = (2.69\times10^5)\, n^{3/2} A D^{1/2} C v^{1/2} \qquad (1)$$

where i_p is the peak current (A), n is the number of electrons transferred ($Fe^{3+} \rightarrow Fe^{2+}$, $n = 1$), A is the effective area of the electrode (cm^2), D is the diffusion coefficient of $[Fe(CN)_6]^{3-}$ (taken to be $7.60 \times 10^{-5} cm^2 s^{-1}$), C is the concentration ($molcm^{-3}$), v is the scan rate (Vs^{-1}).

For detecting ctRNA, 5 µL of magnetically isolated target ctRNA were adsorbed directly onto the GO-$NPFe_2O_3$ modified SPCE followed by the 10 min incubation to attach ctRNA onto the graphene oxide moiety of GO-$NPFe_2O_3$. The electrode was then incubated with 50 µL of 50 µM $[Ru(NH_3)_6]$ for 20 min and washed twice with the PBS. The chronocoulometry (CC) measurement was carried out in 10 mM Tris buffer (pH 7.4) under conditions described previously.[22]. In the case of redox cycle; the CC data was obtained by using 10 mM Tris buffer with 4 mM potassium ferricyanite solution $[Fe(CN)_6]^{3-}$. The number of cationic redox molecules electrostatically associated with the surface-attached anionic phosphate backbone provides a measure of the amount of ctRNA adsorbed onto the GO-$NPFe_2O_3$/SPCE surface. The total charge Q at a time 't' can be expressed by the integrated Cottrell equation (eq. 2) as described previously. [22]

$$Q = \frac{2nFAD_0^{1/2}C_0^*}{\pi^{1/2}} t^{1/2} + Q_{dl} + nFA\Gamma_0 \qquad (2)$$

The amount of RuHex close to electrode surface is denoted by Γ_o while charge obtained by the adsorption of target RNA, also known as surface excess, is represented by $nFA\Gamma_o$. CC curves were constructed by plotting the charge flowing through the ctRNA-attached electrode versus square-root of time ($t^{1/2}/s^{1/2}$). Q and Q_{dl} were estimated from the intercepts of the two curves at t = 0 for the RuHex-treated (i.e., ctRNA-attached electrode was incubated with 50 µM RuHex for 20 min) and untreated (i.e., in the absence of RuHex) electrodes respectively. Therefore, Q represents the total charge comprising both the Faradic and non-Faradic (capacitive) charges. The corresponding charge of RuHex (electrostatically bound to surface confined RNA) and the surface density of ctRNA can be calculated by the eqn (3) and (4), respectively.[14a]

$$Q_{ctRNA} = Q - Q_{dl} \qquad (3)$$

$$\Gamma_o = (Q_{RNA}\, N_A/nFA)(z/m) \qquad (4)$$

where, n is the number of electrons involved in the reaction (n = 1), A is the working electrode area, N_A is the Avogadro's number, m is the number of nucleotides in the ctRNA, and z is the charge of redox molecules (for RuHex, z = 3).

For Fig 3, using the equation (3) and (4), the surface density of ctRNA on the electrode surface were calculated to be 3.57×10^{13} and 5.74×10^{12} molecules cm^{-2} for 1.0 nM and 1.0 fM of ctRNA respectively.

Quantitative Reverse-Transcription Polymerase Chain Reaction (RT-qPCR)

First strand cDNA synthesis was performed using miScript Reverse Transcription kit (Qiagen, Germany). SensiFAST™ SYBR® No-ROX Kit (Biloine, UK) and gene specific primers (Table S1) were used for RT-qPCR analysis. Each qPCR reaction was performed in a total volume of 20µl and contained approx.100-150 ng of cDNA template and 10 µM each of forward and reverse primers. qPCR for fusion gene was performed on CFX96 (Bio-Rad) thermocycler with the following conditions; initial denaturation 95 °C for 2 min followed by 40 cycles of 95 °C for 10 s, 47°C for 30 s, and 72 °C for 20 s (extension). The expression level of fusion gene was normalized against the GAPDH housekeeping gene (qPCR annealing temperature 55 °C). All samples were run in triplicate and no-template control was included in each assay.

Results and discussion

Assay principle

Using FGFR2:FAM76A as a model we report here an amplification-free assay for detecting fusion gene ctRNAs from clinical plasma samples with high detection sensitivity and specificity. The assay principle is schematically outlined in Fig. 1 and described in detail in

experimental section. Target RNAs were hybridized with complementary biotinylated probes. Target-probe hybrids were captured through streptavidin coated magnetic beads followed by magnetic isolation and heat release of captured ctRNAs. The released FGFR2:FAM76A ctRNA were allowed to adsorb onto the GO-NPFe_2O_3 modified screen-printed carbon electrode (SPCE/ GO-NPFe_2O_3) *via* RNA-graphene affinity interaction. This adsorption process follows conventional physisorption mechanism and involves the direct interaction of nucleotides with graphene oxide surface through van der Waal (vdW) forces,[14d, 23] where the interaction between the individual nucleobases and the graphene (i.e., adsorption on graphene) is controlled by the polarizabilities of the nucleobases.[23-24-] In order to quantify the amount of adsorbed FGFR2:FAM76A ctRNA, GO-NPFe_2O_3 modified electrode surface was interrogated in chronocoulometric analyses with $[Ru(NH_3)_6]^{3+}$. The $[Ru(NH_3)_6]^{3+}$acts as a promising indicator for measuring the amount of nucleic acid (e.g., DNA, RNA) on the electrode surface due to its electrostatic affinity for the phosphate groups of the RNA backbone. Improved signal amplification was achieved by coupling $[Ru(NH_3)_6]^{3+}$ system to $[Fe(CN)_6]^{4-/3-}$ redox system as a known signaling molecule for quantification of surface-bound nucleotide on electrodes.[25] Due to chemical oxidation of $Ru(NH_3)_6]^{2+}$ to $[Ru(NH_3)_6]^{3+}$ in mediating $[Fe(CN)_6]^{3-}$, multiple turnovers of $[Ru(NH_3)_6]^{3+}$ resulted in significant signal amplification. Thus, the amount of CC charge generated by the redox couple comprising $[Ru(NH_3)_6]^{3+}$ and $[Fe(CN)_6]^{3-}$ system should have a clear correlation with the concentration of ctRNA. As schematically shown in Fig. 1, target ctRNA absorbed on modified electrode in the presence of electrocatalytic cycle generates higher CC charge (*i.e.* charge density/μCcm^{-2}).

Effect of electrode surface modification

To evaluate the effect of nanoparticles, we investigated our assay with the same amount of FGFR2:FAM76A ctRNA (10 pM) using GO-NPFe_2O_3-modified and unmodified-SPCE (bare

electrode). As can be seen in Fig. 2 and Fig S2, negligible amount of total charge density ($Q/\mu Ccm^{-2}$) was obtained from bare SPCE (SPCE/Bare). This data indicates that there was very insignificant adsorption of target ctRNAs as well as Ru^{3+} onto the bare SPCE electrode. The negligible amount of charge observed in our experiment was probably due to the non-faradic component of the response at the electrode. In a control experiment (Control; SPCE/NPs/PBS), almost 3-times higher total charge was obtained at the GO-NPFe_2O_3-modified SPCE electrode (6.0 versus 2.2 μCcm^{-2}) (Fig. S2). The relatively larger Q at the GO-NPFe_2O_3-modified SPCE can be explained by the fact that the presence of GO-NPFe_2O_3 on the surface of the SPCE could facilitate the adsorption of some redox molecules ($[Ru(NH_3)_6]^{3+}$) that could be electrochemically reduced at the GO-NPFe_2O_3/SPCE electrode.[14a] After the adsorption of target FGFR2:FAM76A ctRNA onto the GO-NPFe_2O_3-modified SPCE, we performed our assay in absence (ctRNA/GO-NPFe_2O_3/SPCE was not incubated with $[Ru(NH_3)_6]^{3+}$) and presence (ctRNA/GO-NPFe_2O_3/SPCE was incubated with $[Ru(NH_3)_6]^{3+}$) of $[Ru(NH_3)_6]^{3}$+. In the absence of $[Ru(NH_3)_6]^{3+}$ (referred as Q_{dl}, e.g., SPCE/NP/mRNA), 10 pM of target ctRNA resulted an approximately 5.2 μCcm^{-2} of charge. In the presence of $[Ru(NH_3)_6]^{3+}$ this value was calculated to be 16.2 μCcm^{-2}. This is could be explained by the fact that, in presence of $[Ru(NH_3)_6]^{3+}$, a stoichiometric amount of Ru^{3+} were bound with the phosphate backbone of surface attached ctRNA and thus an equivalent amount of CC charge was generated.

Specificity of the assay

To assess the assay specificity and efficiency of capture probe for isolating FGFR2:FAM76A ctRNA, we also performed our assay using a noncomplementary FAM-134B mRNA (i.e., SPCE/NP/ FAM-134B mRNA). As can be seen in Figures 2 and S2, a very small increase in the charge density was obtained for FAM-134B mRNA when compared to the control data

(e.g. 6.6 versus 6.0 μCcm^{-2} Fig S2), indicating that our assay is not significantly affected by non-specific mRNAs binding present in the samples. Notably, 10 pM of target ctRNA generated approximately three-times higher charge than that of non-complementary FAM-134B (16.2 versus 6.6 μCcm^{-2}). These data clearly demonstrated the high specificity of our assay in isolating and subsequent electrochemical detection of fusion genes. Most of the conventional biosensors involve hybridization of target to the complementary probes bound to the surface of electrodes. However, interference from non-specific molecules is one the major shortcomings of such a two-dimensional capture approach. In comparison, our assay relies on selective capture of target RNA through complementary probes followed by magnetic bead-based isolation. Intimate mixing of target-probe hybrids with magnetic beads enhances the efficiency of capture. On the other hand, washing, and purification steps avoid matrix effect of complex biological samples and thus reduce non-specific interferences.

Effect of electrocatalytic signal amplification

To enhance the sensitivity of our assay, we coupled the $[Ru(NH_3)_6]^{3+}$ redox system with another redox system, $[Fe(CN)_6]^{3-}$, and measured the amount of CC charges corresponding to the surface-bound ctRNA. $[Ru(NH_3)_6]^{3+}/[Fe(CN)_6]^{3-}$ is a widely used redox system to achieve sensitive electrochemical detection of biomolecules.[18b, 26] In this system, $[Ru(NH_3)_6]^{3+}$ acts as an electron acceptor and is thereby reduced at the electrode surface under the applied reduction potential. The $[Fe(CN)_6]^{3-}$ present in the bulk solution re-oxidized (as $[Fe(CN)_6]^{3-}$ acts as a stronger oxidant in the system) the $[Ru(NH_3)_6]^{2+}$ back to the $[Ru(NH_3)_6]^{3+}$, resulting in the generation of enhanced electrocatalytic signal.[22] As can be seen in Fig. 2, in the presence of $[Ru(NH_3)_6]^{3+}/[Fe(CN)_6]^{3-}$ system the Control (SPCE/NP/Buffer) electrode generated higher amount of charge when compare to that of without electrocatalytic system (20.0 versus 6.0

μCcm^{-2}). The noncomplementary FAM-134B mRNA and Q_{dl} generated almost similar charge responses to that of the Control. For target ctRNA, approximately four-time higher charge density was obtained under electro-catalytic system (63.0 versus 16.2 μCcm^{-2}) than what was observed in the absence of $[Fe(CN)_6]^{3-}$. It is also worth mentioning that a significant enhancement in CC response was found with the electrocatalytic system (Control vs target mRNA, 20.0 versus 63 μCcm^{-2} in Fig 2) compared to that without electrocatalytic cycle (Control vs target mRNA, 6.0 versus 16.2 μCcm^{-2} in Fig. S2). This high signal responses of the target mRNA compared to controls and non-specific mRNA clearly demonstrate the enhanced functionality and specificity of our assay.

Sensitivity of the assay

To test the sensitivity and reproducibility of our assay, various concentrations of synthetic target RNA ranging from 1.0 fM to 1.0 nM were adsorbed onto the GO-NPFe_2O_3-modified electrode surface (Fig. 3). As shown in Fig. 3A, the CC charge generated by $[Ru(NH_3)_6]^{3+}/[Fe(CN)_6]^{3-}$ electrocatalytic cycle increases with increasing RNA concentration. In comparison, negligible signal was observed in the No-Target (NoT) control experiment. The linear regression equation was calculated to be *y* (charge density, μCcm^{-2}) = 8.047 (amount of RNA) + 0.1134, with a correlation coefficient (R^2) of 0.97154 (Fig. 3B). The limit of detection (LOD) was estimated to be 1 fM which is clearly distinguishable from that of control electrode. Without the catalytic cycle step (i.e., using only $[Ru(NH_3)_6]^{3+}$), we obtained 100 times less sensitive LOD (1 fM versus 100 fM) (Fig. S3A). For the system without the catalytic cycle step, the linear regression equation was estimated to be y (charge density, μCcm^{-2}) = 4.147 (amount of RNA) + 1.0106, with a correlation coefficient (R^2) of 0.99773 (S3B).

The high sensitivity of our assay may be attributed to the large exposed surface area of graphene oxide within the GO-$NPFe_2O_3$ nanoparticles, which leads to a relatively larger amount of RNA being adsorbed onto the GO-$NPFe_2O_3$-modified SPCE via the RNA-graphene oxide affinity interaction. This also allows a relatively larger amount of $[Ru(NH^3)^6]^{3+}$ ions to be electrostatically bound to surface confined RNA. Moreover, GO-$NPFe_2O_3$ nanoparticles can increase electrocatalytic signal of Ru^{3+}/Ru^{2+} process. The LOD of our method is higher than some of the earlier electrochemical fusion gene assays.[17b, 27] Although some other studies have reported similar LODs (Table S2) the usage of these methods is hindered mainly because they involve enzyme-based amplification[28] and complicated surface functionalization steps (the extra steps involved in the immobilization and hybridization of DNA probes on electrodes for capturing target DNA),[29] or both of them.[30] It is also important to note that only a few electrochemical methods can offer relatively higher sensitivity.[31] However, clinical application of these methods may also be restricted due to the complexities in sensor fabrication steps. In contrast to these, our assay is relatively simple and does not require any immobilization of probe on the electrode surface and thus simplifies the detection method by avoiding the complex chemistry underlying each step of the sensor fabrication.

FGFR2:FAM76A ctRNA detection in clinical plasma samples

To assess the applicability of our assay in analyzing complex clinical samples, we used this amplification-free electrochemical method for the analysis of FGFR2:FAM76A ctRNA levels in total RNA extracted from the clinical plasma samples of 5 HG-SC (P1- P5), and 5 benign patients for ovarian cancer as controls (B1-B5). Our assay detected all the cancer samples to be FGFR2:FAM76A positive, and CC signals generated by our assay could distinguish different FGFR2:FAM76A levels in clinical samples as depicted in Fig. 4A. The FGFR2:FAM76A -positive samples showed higher CC charge density as compared to benign

samples, which indicates upregulation of FGFR2:FAM76A in ovarian cancer patients. These clinical data represents a very good reproducibility of our assay (relative standard deviation, % RSD = < 5%, for n = 3) for analyzing differential expression pattern of FGFR2:FAM76A genes in ovarian cancer sample. We also validated the results of our electrochemical analysis by determining expression of FGFR2:FAM76A fusion gene in a subset of clinical samples through standard RT-qPCR method. Fusion gene expression was normalized against the expression of GAPDH and data is presented as Δ_{cq}. As can be seen in Figure 4B, qPCR results show a trend similar to those of electrochemical analysis, demonstrating the accuracy and potential of our assay.

Furthermore, results of our assay were also consistent with published reports describing the presence of FGFR2:FAM76A in ovarian cancer patients.[7] The clinical significance of our assay is broad, as it is useful for detecting different gene fusions in RNA/DNA by changing the capture probe sequences, which will pave the way for comprehensive diagnosis and personalized treatment. The assay is a portable, cost affordable, non-enzymatic and amplification-free alternative to current amplification-based approaches for fusion gene detection. This method avoids PCR, which is prone to sequence specific amplification biases and requires sample preprocessing, thus significantly increasing cost and time of the analysis. Our method removes complicated cleaning and sensor fabrication, tedious experimental protocols, and costly fluorescence readout instruments. In addition, our method uses commercially available and disposable SPCE electrodes, which are cheap and avoid the utilization of typical electrochemical cells, counter and reference electrodes thereby providing a relatively simple platform with highly reproducible results. Most importantly, the method uses GO-NPFe_2O_3 nanoparticles to modify electrode. Due to the synergistic effects of Fe_3O_4 nanoparticles and graphene with a large surface area and excellent electron transfer ability, the obtained nanocomposite significantly improves the sensing behavior for RNA detection.

Owing to the sensitivity, simplicity, inexpensive and portable nature of our method, the proposed approach is ideal for developing a clinically friendly FGFR2:FAM76A assay.

Conclusions

We have presented the first amplification-free and enzyme-free electrochemical assay for the detection of FGFR2:FAM76A ctNAs using a new class of iron oxide nanoparticles. The assay demonstrates a high sensitivity due to (i) high surface area and catalytic activity of GO-NPFe_2O_3 nanoparticles and (ii) the use of the $[Ru(NH_3)_6]^{3+}$/ $[Fe(CN)_6]^{3-}$ electrocatalytic cycle for signal amplification. Moreover, this method involves a good level of specificity due to functionalized magnetic dynabeads based target capture. We successfully examined the assay performance in clinical samples obtained from benign and high-grade ovarian cancer patients, with good reproducibility (% RSD = <5%, for n = 3). We envisage that due to its flexibility, our method may find broad application in ctNA based fusion gene detection in a variety of cancers.

Acknowledgements

This work was supported by the NHMRC CDF (APP1088966 to M.J.A.S.) and higher degree research scholarships (GUIPRS and GUPRS scholarships to L.G) from the Griffith University. N.T.N and M.J.A.S acknowledge funding support from Australian Research Council's grant DP180100055. C.S. is supported by The Lions Medical Research Foundation (LMRF), Ovarian Cancer Research Foundation (OCRF) and and Fondo Nacional de Desarrollo Científico y Tecnológico (FONDECYT 1170809).

References

[1] A. M. Newman, S. V. Bratman, J. To, J. F. Wynne, N. C. W. Eclov, L. A. Modlin, C. L. Liu, J. W. Neal, H. A. Wakelee, R. E. Merritt, J. B. Shrager, B. W. Loo Jr, A. A. Alizadeh, M. Diehn, *Nat. Med.* **2014**, *20*, 548.

[2] a) E. Heitzer, P. Ulz, J. B. Geigl, *Clin. Chem.* **2015**, *61*, 112-123; b) H. Schwarzenbach, D. S. B. Hoon, K. Pantel, *Nature Reviews Cancer* **2011**, *11*, 426.

[3] F. Mertens, B. Johansson, T. Fioretos, F. Mitelman, *Nature Reviews Cancer* **2015**, *15*, 371.

[4] C. Tognon, S. R. Knezevich, D. Huntsman, C. D. Roskelley, N. Melnyk, J. A. Mathers, L. Becker, F. Carneiro, N. MacPherson, D. Horsman, C. Poremba, P. H. B. Sorensen, *Cancer Cell* **2002**, *2*, 367-376.

[5] M. Soda, Y. L. Choi, M. Enomoto, S. Takada, Y. Yamashita, S. Ishikawa, S.-i. Fujiwara, H. Watanabe, K. Kurashina, H. Hatanaka, M. Bando, S. Ohno, Y. Ishikawa, H. Aburatani, T. Niki, Y. Sohara, Y. Sugiyama, H. Mano, *Nature* **2007**, *448*, 561.

[6] K. M. Koo, L. G. Carrascosa, M. J. A. Shiddiky, M. Trau, *Anal. Chem.* **2016**, *88*, 6781-6788.

[7] J. A. Martignetti, O. Camacho-Vanegas, N. Priedigkeit, C. Camacho, E. Pereira, L. Lin, L. Garnar-Wortzel, D. Miller, B. Losic, H. Shah, J. Liao, J. Ma, P. Lahiri, M. Chee, E. Schadt, P. Dottino, *Neoplasia* **2014**, *16*, 97-103.

[8] A. McPherson, F. Hormozdiari, A. Zayed, R. Giuliany, G. Ha, M. G. F. Sun, M. Griffith, A. Heravi Moussavi, J. Senz, N. Melnyk, M. Pacheco, M. A. Marra, M. Hirst, T. O. Nielsen, S. C. Sahinalp, D. Huntsman, S. P. Shah, *PLoS Comput. Biol.* **2011**, *7*, e1001138.

[9] J. Salzman, R. J. Marinelli, P. L. Wang, A. E. Green, J. S. Nielsen, B. H. Nelson, C. W. Drescher, P. O. Brown, *PLoS Biol.* **2011**, *9*, e1001156.

[10] K. Kannan, C. Coarfa, K. Rajapakshe, S. M. Hawkins, M. M. Matzuk, A. Milosavljevic, L. Yen, *PLoS Genet.* **2014**, *10*, e1004216.

[11] C. Bettegowda, M. Sausen, R. J. Leary, I. Kinde, Y. Wang, N. Agrawal, B. R. Bartlett, H. Wang, B. Luber, R. M. Alani, E. S. Antonarakis, N. S. Azad, A. Bardelli, H. Brem, J. L. Cameron, C. C. Lee, L. A. Fecher, G. L. Gallia, P. Gibbs, D. Le, R. L. Giuntoli, M. Goggins, M. D. Hogarty, M. Holdhoff, S.-M. Hong, Y. Jiao, H. H. Juhl, J. J. Kim, G. Siravegna, D. A. Laheru, C. Lauricella, M. Lim, E. J. Lipson, S. K. N. Marie, G. J. Netto, K. S. Oliner, A. Olivi, L. Olsson, G. J. Riggins, A. Sartore-Bianchi, K. Schmidt, l.-M. Shih, S. M. Oba-Shinjo, S. Siena, D. Theodorescu, J. Tie, T. T. Harkins, S. Veronese, T.-L. Wang, J. D. Weingart, C. L. Wolfgang, L. D. Wood, D. Xing, R. H. Hruban, J. Wu, P. J. Allen, C. M. Schmidt, M. A. Choti, V. E. Velculescu, K. W. Kinzler, B. Vogelstein, N. Papadopoulos, L. A. Diaz, *Sci. Transl. Med.* **2014**, *6*, 224ra224-224ra224.

[12] M. Murtaza, S.-J. Dawson, D. W. Y. Tsui, D. Gale, T. Forshew, A. M. Piskorz, C. Parkinson, S.-F. Chin, Z. Kingsbury, A. S. C. Wong, F. Marass, S. Humphray, J. Hadfield, D. Bentley, T. M. Chin, J. D. Brenton, C. Caldas, N. Rosenfeld, *Nature* **2013**, *497*, 108.

[13] A. R. Thierry, F. Mouliere, S. El Messaoudi, C. Mollevi, E. Lopez-Crapez, F. Rolet, B. Gillet, C. Gongora, P. Dechelotte, B. Robert, M. Del Rio, P.-J. Lamy, F. Bibeau, M. Nouaille, V. Loriot, A.-S. Jarrousse, F. Molina, M. Mathonnet, D. Pezet, M. Ychou, *Nat. Med.* **2014**, *20*, 430.

[14] a) M. Kamal Masud, M. N. Islam, M. H. Haque, S. Tanaka, V. Gopalan, G. Alici, N.-T. Nguyen, A. K. Lam, M. S. A. Hossain, Y. Yamauchi, M. J. A. Shiddiky, *Chem. Commun.* **2017**, *53*, 8231-8234; b) M. N. Islam, V. Gopalan, M. H. Haque, Mostafa K. Masud, M. S. A. Hossain, Y. Yamauchi, N.-T. Nguyen, A. K.-Y. Lam, M. J. A. Shiddiky, *Biosensors Bioelectron.* **2017**, *98*, 227-233; c) M. H. Haque, V. Gopalan, M. N. Islam, M. K. Masud, R. Bhattacharjee, M. S. A. Hossain, N.-T. Nguyen, A. K. Lam, M. J. A. Shiddiky, *Anal. Chim. Acta* **2017**, *976*, 84-93; d) M. H. Haque, V. Gopalan, S. Yadav, M. N. Islam, E. Eftekhari, Q. Li, L. G. Carrascosa, N.-T. Nguyen, A. K. Lam, M. J. A. Shiddiky, *Biosensors Bioelectron.* **2017**, *87*, 615-621; e) F. Islam, M. H. Haque, S. Yadav, M. N. Islam, V. Gopalan, N.-T. Nguyen, A. K. Lam, M. J. A. Shiddiky, *Sci. Rep.* **2017**, *7*, 133.

[15] C.-Y. Hong, X. Chen, T. Liu, J. Li, H.-H. Yang, J.-H. Chen, G.-N. Chen, *Biosensors Bioelectron.* **2013**, *50*, 132-136.

[16] Y. Wen, H. Pei, Y. Shen, J. Xi, M. Lin, N. Lu, X. Shen, J. Li, C. Fan, *Sci. Rep.* **2012**, *2*, 867.
[17] a) Y. Chu, B. Cai, Y. Ma, M. Zhao, Z. Ye, J. Huang, *RSC Advances* **2016**, *6*, 22673-22678; b) T. Wang, R. Zhu, J. Zhuo, Z. Zhu, Y. Shao, M. Li, *Anal. Chem.* **2014**, *86*, 12064-12069.
[18] a) J. Das, I. Ivanov, E. H. Sargent, S. O. Kelley, *J Am Chem Soc* **2016**, *138*, 11009-11016; b) J. Das, I. Ivanov, L. Montermini, J. Rak, E. H. Sargent, S. O. Kelley, *Nat. Chem.* **2015**, *7*, 569.
[19] a) K. M. Koo, B. McNamara, E. J. H. Wee, Y. Wang, M. Trau, *J. Biomed. Nanotechnol.* **2016**, *12*, 1798-1805; b) K. M. Koo, E. J. H. Wee, P. N. Mainwaring, M. Trau, *Sci. Rep.* **2016**, *6*, 30722.
[20] S. Tanaka, R. R. Salunkhe, Y. V. Kaneti, V. Malgras, S. M. Alshehri, T. Ahamad, M. B. Zakaria, S. X. Dou, Y. Yamauchi, M. S. A. Hossain, *RSC Advances* **2017**, *7*, 33994-33999.
[21] M. J. A. Shiddiky, A. A. J. Torriero, C. Zhao, I. Burgar, G. Kennedy, A. M. Bond, *J Am Chem Soc* **2009**, *131*, 7976-7989.
[22] M. N. Islam, M. K. Masud, N.-T. Nguyen, V. Gopalan, H. R. Alamri, Z. A. Alothman, M. S. A. Hossain, Y. Yamauchi, A. K. Lamd, M. J. A. Shiddiky, *Biosensors Bioelectron.* **2018**, *101*, 275-281.
[23] S. Gowtham, H. S. Ralph, P. Ravindra, P. K. Shashi, A. Rajeev, *Nanotechnology* **2008**, *19*, 125701.
[24] M. Wu, R. Kempaiah, P.-J. J. Huang, V. Maheshwari, J. Liu, *Langmuir* **2011**, *27*, 2731-2738.
[25] A. A. I. Sina, S. Howell, L. G. Carrascosa, S. Rauf, M. J. A. Shiddiky, M. Trau, *Chem. Commun.* **2014**, *50*, 13153-13156.
[26] R. Gasparac, B. J. Taft, M. A. Lapierre-Devlin, A. D. Lazareck, J. M. Xu, S. O. Kelley, *J Am Chem Soc* **2004**, *126*, 12270-12271.
[27] a) A. Sharma, C. M. Pandey, G. Sumana, U. Soni, S. Sapra, A. K. Srivastava, T. Chatterjee, B. D. Malhotra, *Biosensors Bioelectron.* **2012**, *38*, 107-113; b) A. Sharma, G. Sumana, S. Sapra, B. D. Malhotra, *Langmuir* **2013**, *29*, 8753-8762.
[28] L. Hu, T. Tan, G. Chen, K. Zhang, J.-J. Zhu, *Electrochem. Commun.* **2013**, *35*, 104-107.
[29] J. Yang, W. Zhang, *J. Solid State Electrochem.* **2014**, *18*, 2863-2868.
[30] K. Wang, J. Chen, J. Chen, A. Liu, G. Li, H. Luo, X. Lin, Y. Chen, *Electroanalysis* **2009**, *21*, 1159-1166.
[31] a) C. M. Pandey, S. Dewan, S. Chawla, B. K. Yadav, G. Sumana, B. D. Malhotra, *Anal. Chim. Acta* **2016**, *937*, 29-38; b) K. Y. P. S. Avelino, I. A. M. Frias, N. Lucena-Silva, R. G. Gomes, C. P. de Melo, M. D. L. Oliveira, C. A. S. Andrade, *Colloids Surf. B. Biointerfaces* **2016**, *148*, 576-584.
[32] L. Wang, E. Hua, M. Liang, C. Ma, Z. Liu, S. Sheng, M. Liu, G. Xie, W. Feng, *Biosensors Bioelectron.* **2014**, *51*, 201-207.

Figures

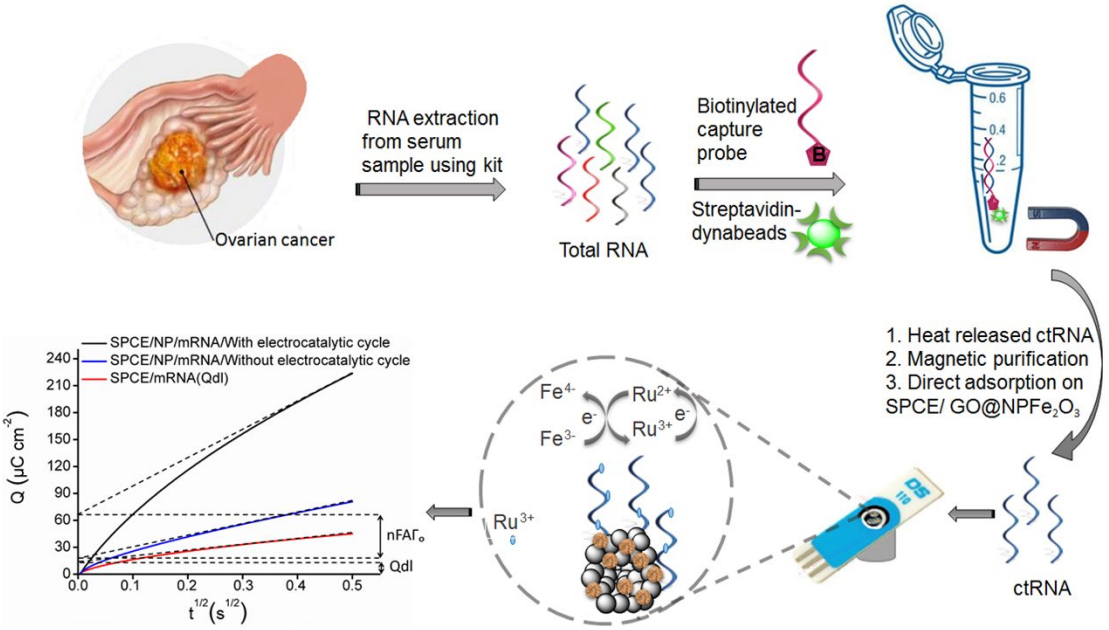

Fig. 1 Assay principle for quantification of ctRNA. Total cell-free RNA was extracted from plasma sample using a commercially available kit. Target fusion gene ctRNA was separated and purified magnetically from the bulk of RNA and adsorbed directly on the GO-$NPFe_2O_3$ modified screen-printed carbon electrode (SPCE). A significant electrocatalytic signal amplification was attained via the chronocoulometric (CC) charge interrogation of target ctRNA-bound $[Ru(NH3)_6]^{3+}$- $[Fe(CN)_6]^{3-}$ electrocatalytic assay system. Inset: typical electrocatalytic cycle showing the electrostatically attached target ctRNA that generates higher CC charge in comparison to without electrocatalytic cycle.

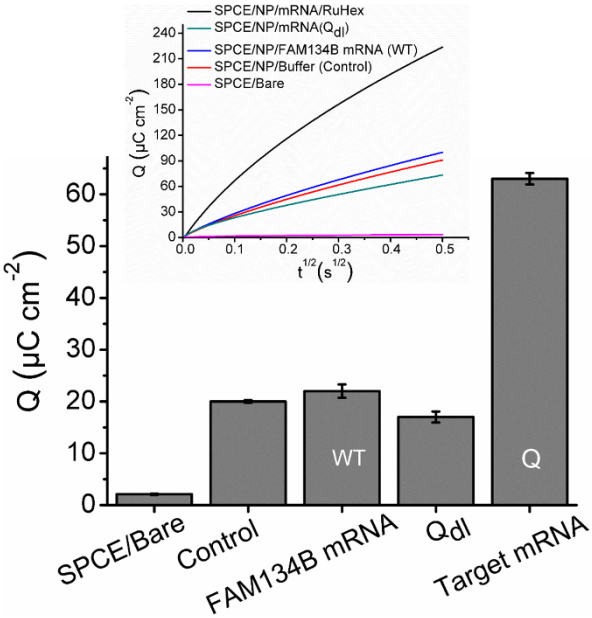

Fig. 2 Specificity of the Assay. Charge density data for SPCE/Bare (without NP modification), control (i.e., NP modified electrode without RNA), Q_{dl}- the non-Faradic charge in the absence of RuHex, non-complementary FAM-134B, target mRNA (ctRNA) Inset; corresponding CC curves (Q vs. $t^{1/2}$). Each data point represents the average of three independent trials, and error bars represent the standard deviation of measurements (% RSD = <5%, for n = 3).

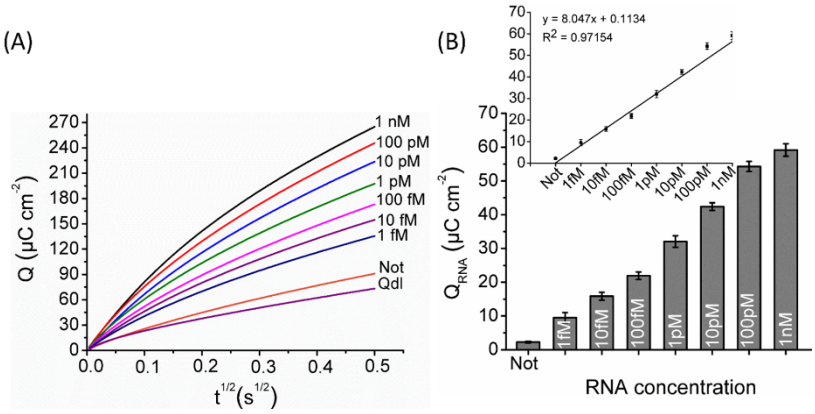

Fig. 3 (A). Typical CC curves (Q vs. $t^{1/2}$) for the 1.0 fM-1.0 nM of synthetic ctRNA (with $[Ru(NH3)_6]^{3+}$- $[Fe(CN)_6]^{3-}$ electrocatalytic assay system) . (B) Corresponding calibration plot. Q_{ctRNA} (corresponding charge of target ctRNA bound to surface bound RuHex) = Q – Q_{dl}. The concentration of RuHex and ferricyanide is 50 μM and 4.0 mM respectively. Each data point

represents the average of three independent trials, and error bars represent the standard deviation of measurements (% RSD = <5%, for n = 3).

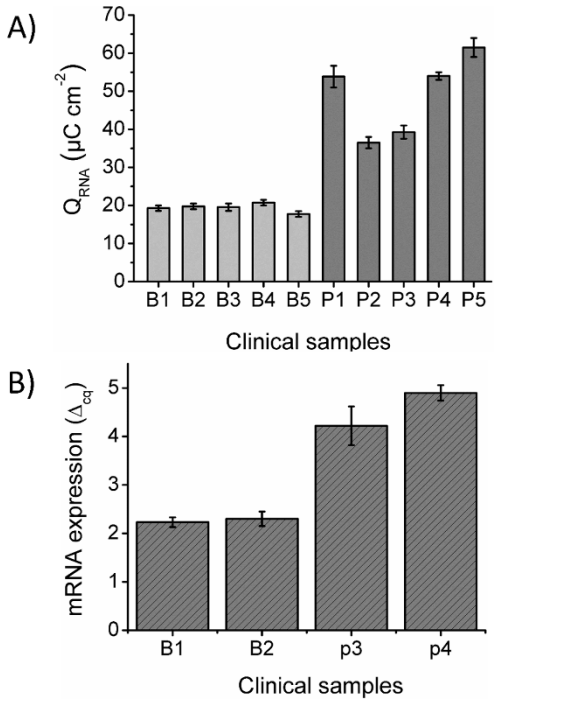

Fig. 4 (A). Analysis of patient samples. Corresponding QRNA obtained for five benign ovarian cancer patients (B1-B5) and five patients of high-grade serous subtype ovarian cancer (P1-P5) (B). RT-qPCR ctRNA expression profile in plasma samples. Each data point represents the average of three independent trials, and error bars represent the standard deviation of measurements (% RSD = <5%, for n = 3).

TOC

FGFR2: FAM76A fusion gene in circulating tumor RNA of ovarian cancer patients is detected by using (*i*) direct adsorption of RNA via graphene-RNA affinity interaction and (*ii*) electrocatalytic signal amplification.

Supplementary materials

Detection of FGFR2: FAM76A fusion gene in circulating tumor RNA based on catalytic signal amplification of graphene oxide-coated magnetic nanoparticles

Lena Gorgannezhad,[a,b] Muhammad Umer,[b] Mostafa Kamal Masud,[c] Yusuke Yamauchi,[d] Shahriar Al Hossain,[c] Carlos Salomon,[e,f,g] Richard Kline, [g] Nam-Trung Nguyen,[b] Muhammad J.A. Shiddiky[a,b*]

[a]*School of Natural Sciences, Griffith University, Nathan Campus, QLD 4111, Australia*

[b]*Queensland Micro- and Nanotechnology Centre, Griffith University, Nathan Campus, QLD 4111, Australia*

[c]*Australian Institute for Innovative Materials (AIIM), University of Wollongong, Squires Way, Innovation Campus, North Wollongong, NSW 2519, Australia*

[d]*International Center for Materials Nanoarchitectonics, National Institute for Materials Science (NIMS), Japan 1-2-1 Sengen, Tsukuba-city, Ibaraki 305-0047, Japan*

[e]*Exosome Biology Laboratory, Centre for Clinical Diagnostics, University of Queensland Centre for Clinical Research, Royal Brisbane and Women's Hospital, The University of Queensland, Brisbane, QLD, Australia*

[f]*Department of Clinical Biochemistry and Immunology, Faculty of Pharmacy, University of Concepción, Concepción, Chile.*

[g]*Maternal-Fetal Medicine, Department of Obstetrics and Gynecology, Ochsner Clinic Foundation, New Orleans, USA.*

*Corresponding author emails: m.shiddiky@griffith.edu.au (MJAS).

List of Contents

1. Supplementary tables

Table S1. List of the oligonucleotide sequences applied in this assay.

Target genes and primers	**Oligonucleotide sequences (5′−3′)**
Synthetic FGFR2- FAM76A Fusion sequence	5′-U-GUA-AAA-CAA-ACA-UAU-GUU-CCU-UUC-CUU-UCA-3′
Biotinylated capture probes of FGFR2- FAM76A Fusion	5′-TGA-AAG-GAA-AGG-AAC-ATA-TGT-TTG-TTT-TAC-A-3′-Biotin
FGFR2- FAM76A Fusion forward	5′-GGATAAAGGAAGAGATTGCAC-3′
FGFR2- FAM76A fusion reverse	5′ TGTGGGAGTTAAGTAAGAACT-3′

Table S2. Some available methodologies for different fusion genes detection.

Method	**Fusion gene**	**LOD**	**References**
Chitosan encapsulated quantum dots platform	BCR-ABL	2.56 pM	27a
Quantum dots self-assembly platform	BCR-ABL	1.0 pM	27b
Graphene sheets, polyaniline and AuNPs based DNA sensor	BCR-ABL	2.11 pM	32
Polymerase assisted multiplication coupling with quantum dot tagging	BCR-ABL	2 fM	28
Indicator-free DNA hybridization biosensor with a graphene-based nanocomposite	BCR-ABL	2.6 fM	29
Controlled deposition of functionalized silica coated zinc oxide nano-assemblies at the air/water interface	CML	1×10^{-16} M	31a
DNA biosensor based on aldehyde-agarose hydrogel modified glassy carbon electrode	BCR-ABL	4.0 pM	31b
A sandwich-type electrochemical biosensor using locked nucleic acids on gold electrode	CML	10 fM	30

2. Supplementary figures

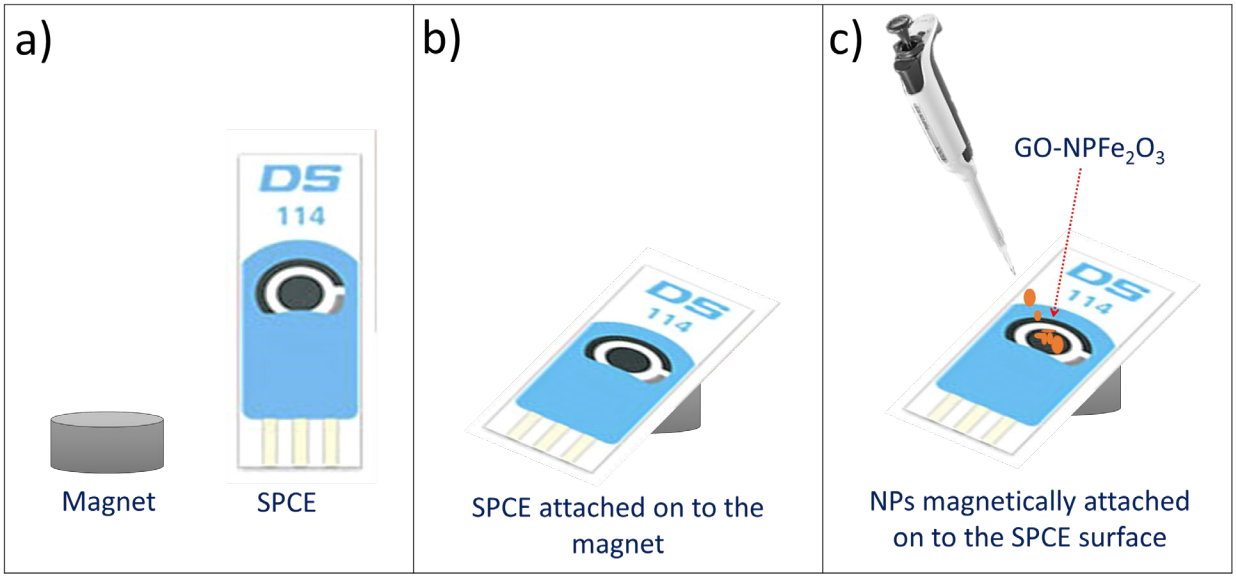

Figure S1: Schematic representation of the electrode preparation. a) The magnet and screen printed carbon electrode (SPCE); b) SPCE centered and attached onto the magnet; and c) the GO-NPFe_2O_3 NPs were attached magnetically onto the SCE surface throughout the whole experiment

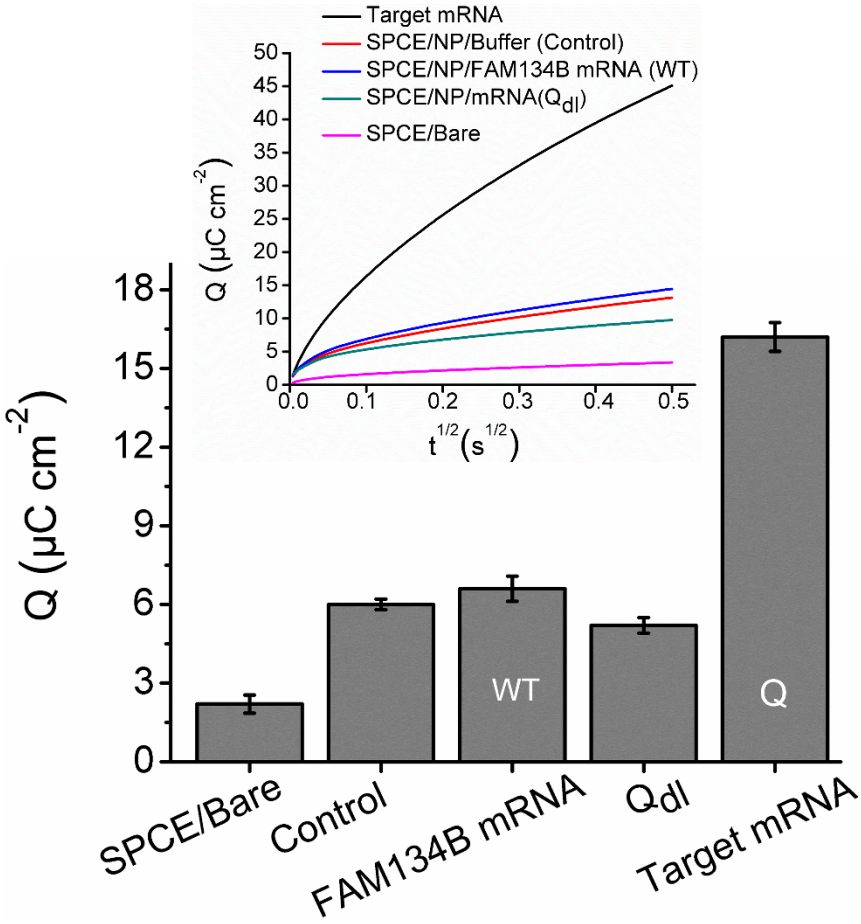

Fig. S2 Specificity of the Assay. Corresponding charge density data without electrocatalytic cycle (in the presence of only [Ru(NH3)6]3+) for the SPCE/Bare (without NP modification), control (i.e., NP modified electrode without RNA), Q_{dl}- the non-Faradic charge in the absence of RuHex; non-complementary FAM-134B, and target mRNA (ctRNA). Inset: corresponding CC curves (Q vs. $t^{1/2}$). Each data point represents the average of three independent trials, and error bars represent the standard deviation of measurements (% RSD = <5%, for n = 3).

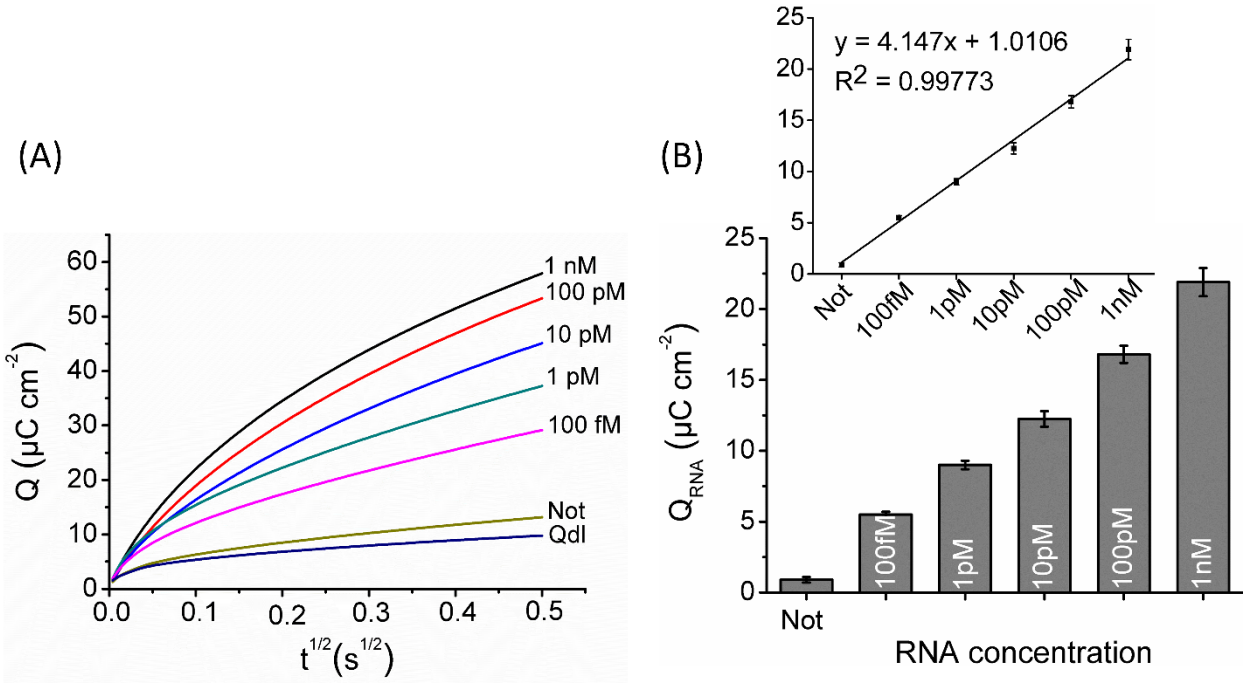

Fig. S3 (A). Typical CC curves (Q vs. $t^{1/2}$) for the 100 fM-1.0 nM of synthetic ctRNA (mRNA) without electrocatalytic cycle. (B) corresponding calibration plot. Q_{ctRNA} (corresponding charge of target ctRNA bound to surface bound RuHex) = Q– Q_{dl}. Each data point represents the average of three independent trials, and error bars represent the standard deviation of measurements (% RSD = <5%, for n = 3).